CHAPTER 16

EXPERIMENTAL STRESS ANALYSIS

Introduction

We live today in a complex world of manmade structures and machines. We work in buildings which may be many storeys high and travel in cars and ships, trains and planes; we build huge bridges and concrete dams and send mammoth rockets into space. Such is our confidence in the modern engineer that we take these manmade structures for granted. We assume that the bridge will not collapse under the weight of the car and that the wings will not fall away from the aircraft. We are confident that the engineer has assessed the stresses within these structures and has built in sufficient strength to meet all eventualities.

This attitude of mind is a tribute to the competence and reliability of the modern engineer. However, the commonly held belief that the engineer has been able to calculate mathematically the stresses within the complex structures is generally ill-founded. When he is dealing with familiar design problems and following conventional practice, the engineer draws on past experience in assessing the strength that must be built into a structure. A competent civil engineer, for example, has little difficulty in selecting the size of steel girder that he needs to support a wall. When he departs from conventional practice, however, and is called upon to design unfamiliar structures or to use new materials or techniques, the engineer can no longer depend upon past experience. The mathematical analysis of the stresses in complex components may not, in some cases, be a practical proposition owing to the high cost of computer time involved. If the engineer has no other way of assessing stresses except by recourse to the nearest standard shape and hence analytical solution available, he builds in greater strength than he judges to be necessary (i.e. he incorporates a factor of safety) in the hope of ensuring that the component will not fail in practice. Inevitably, this means unnecessary weight, size and cost, not only in the component itself but also in the other members of the structure which are associated with it.

To overcome this situation the modern engineer makes use of experimental techniques of stress measurement and analysis. Some of these consist of "reassurance" testing of completed structures which have been designed and built on the basis of existing analytical knowledge and past experience: others make use of scale models to predict the stresses, often before final designs have been completed.

Over the past few years these *experimental stress analysis* or *strain measurement* techniques have served an increasingly important role in aiding designers to produce not only efficient but economic designs. In some cases substantial reductions in weight and easier manufacturing processes have been achieved.

A large number of problems where experimental stress analysis techniques have been of particular value are those involving fatigue loading. Under such conditions failure usually starts when a fatigue crack develops at some position of high localised stress and propagates

until final rupture occurs. As this often requires several thousand repeated cycles of load under service conditions, full-scale production is normally well under way when failure occurs. Delays at this stage can be very expensive, and the time saved by stress analysis techniques in locating the source of the trouble can far outweigh the initial cost of the equipment involved.

The main techniques of experimental stress analysis which are in use today are:

(1) brittle lacquers
(2) strain gauges
(3) photoelasticity
(4) photoelastic coatings

The aim of this chapter is to introduce the fundamental principles of these techniques, together with limited details of the principles of application, in order that the reader can appreciate (a) the role of the experimental techniques as against the theoretical procedures described in the other chapters, (b) the relative merits of each technique, and (c) the more specialised literature which is available on the techniques, to which reference will be made.

16.1. Brittle lacquers

The brittle-lacquer technique of experimental stress analysis relies on the failure by cracking of a layer of a brittle coating which has been applied to the surface under investigation. The coating is normally sprayed onto the surface and allowed to air- or heat-cure to attain its brittle properties. When the component is loaded, this coating will crack as its so-called *threshold strain* or *strain sensitivity* is exceeded. A typical crack pattern obtained on an engineering component is shown in Fig. 16.1. Cracking occurs where the strain is greatest,

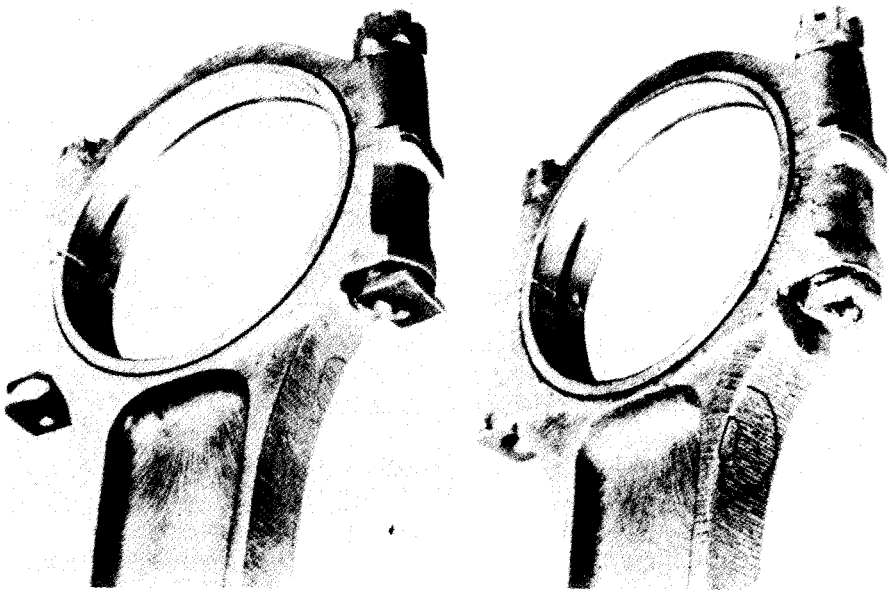

Fig. 16.1. Typical brittle-lacquer crack pattern on an engine con-rod. (Magnaflux Corporation.)

so that an immediate indication is given of the presence of stress concentrations. The cracks also indicate the directions of maximum strain at these points since they are always aligned at right angles to the direction of the maximum principal tensile strain. The method is thus of great value in determining the optimum positions in which to place strain gauges (see §16.2) in order to record accurately the measurements of strain in these directions.

The brittle-coating technique was first used successfully in 1932 by Dietrich and Lehr in Germany despite the fact that references relating to observation of the phenomenon can be traced back to Clarke's investigations of tubular bridges in 1850. The most important advance in brittle-lacquer technology, however, came in the United States in 1937–41 when Ellis, De Forrest and Stern produced a series of lacquers known as "Stresscoat" which, in a modified form, remain widely used in the world today.

There are many every-day examples of brittle coatings which can be readily observed by the reader to exhibit cracks indicating local yielding when the strain is sufficiently large, e.g. cellulose, vitreous or enamel finishes. Cellulose paints, in fact, are used by some engineering companies as a brittle lacquer on rubber models where the strains are quite large.

As an interesting experiment, try spraying a comb with several thin coats of hair-spray lacquer, giving each layer an opportunity to dry before application of the next coat. Finally, allow the whole coating several hours to fully cure; cracks should then become visible when the comb is bent between your fingers.

In engineering applications a little more care is necessary in the preparation of the component and application of the lacquer, but the technique remains a relatively simple and hence attractive one. The surface of the component should be relatively smooth and clean, standard solvents being used to remove all traces of grease and dirt. The lacquer can then be applied, the actual application procedure depending on the type of lacquer used. Most lacquers may be sprayed or painted onto the surface, spraying being generally more favoured since this produces a more uniform thickness of coating and allows a greater control of the thickness. Other lacquers, for example, are in wax or powder form and require pre-heating of the component surface in order that the lacquer will melt and run over the surface. Optimum coating thicknesses depend on the lacquer used but are generally of the order of 1 mm.

In order to determine the strain sensitivity of the lacquer, and hence to achieve an approximate idea of the strains existing in the component, it is necessary to coat calibration bars at the same time and in exactly the same manner as the specimen itself. These bars are normally simple rectangular bars which fit into the calibration jig shown in Fig. 16.2 to form a simple cantilever with an offset cam at the end producing a known strain distribution along the cantilever length. When the lacquer on the bar is fully cured, the lever on the cam is moved forward to depress the end of the bar by a known amount, and the position at which the cracking of the lacquer begins gives the strain sensitivity when compared with the marked strain scale. This enables quantitative measurements of strain levels to be made on the components under test since if, for example, the calibration sensitivity is shown to be 800 microstrain (strain $\times 10^{-6}$), then the strain at the point on the component at which cracks first appear is also 800 microstrain.

This type of quantitative measurement is generally accurate to no better than 10–20 %, and brittle-lacquer techniques are normally used to locate the *positions* of stress maxima, the actual values then being determined by subsequent strain-gauge testing.

Loading is normally applied to the component in increments, held for a few minutes and released to zero prior to application of the next increment; the time interval between increments should be several times greater than that of the loading cycle. With this procedure

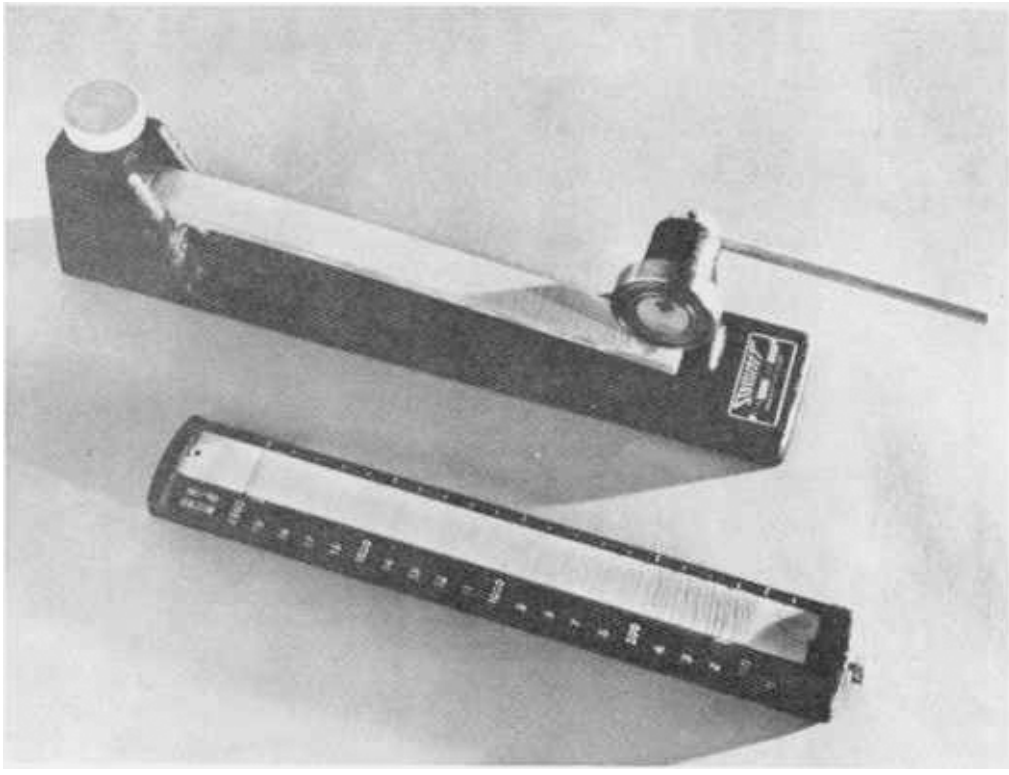

Fig. 16.2. (*Top*) Brittle-lacquer calibration bar in a calibration jig with the cam depresed to apply load. (*Bottom*) Calibration of approximately 100 microstrain. (Magna-flux Corporation.)

creep effects in the lacquer, where strain in the lacquer changes at constant load, are completely overcome. After each load application, cracks should be sought and, when located, encircled and identified with the load at that stage using a chinagraph pencil. This enables an accurate record of the development of strain throughout the component to be built up.

There are a number of methods which can be used to aid crack detection including (a) pre-coating the component with an aluminium undercoat to provide a background of uniform colour and intensity, (b) use of a portable torch which, when held close to the surface, highlights the cracks by reflection on the crack faces, (c) use of dye-etchants or special electrified particle inspection techniques, details of which may be found in standard reference texts.[3]

Given good conditions, however, and a uniform base colour, cracks are often visible without any artificial aid, viewing the surface from various angles generally proving sufficient.

Figures 16.3 and 16.4 show further examples of brittle-lacquer crack patterns on typical engineering components. The procedure is simple, quick and relatively inexpensive; it can be carried out by relatively untrained personnel, and immediate qualitative information, such as positions of stress concentration, is provided on the most complicated shapes.

Various types of lacquer are available, including a special ceramic lacquer which is

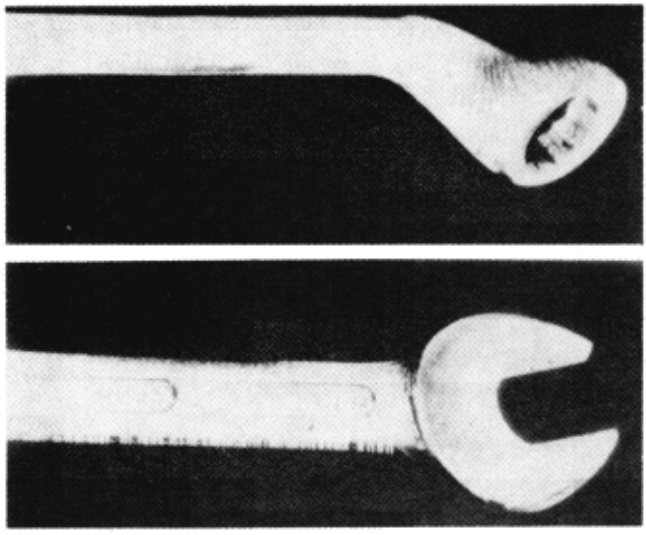

Fig. 16.3. Brittle-lacquer crack patterns on an open-ended spanner and a ring spanner. In the former the cracks appear at right angles to the maximum bending stress in the edge of the spanner whilst in the ring spanner the presence of torsion produces an inclination of the principal stress and hence of the cracks in the lacquer.

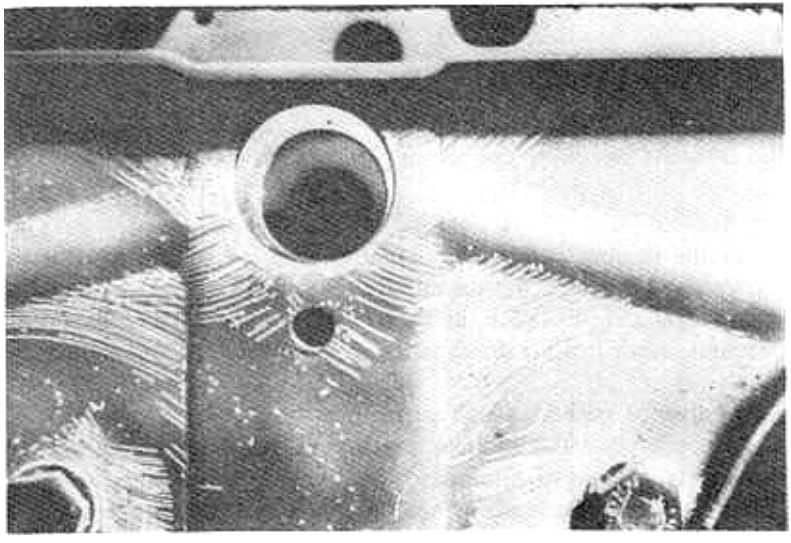

Fig. 16.4. Brittle-lacquer crack pattern highlighting the positions of stress concentration on a motor vehicle component. (Magnaflux Corporation.)

particularly useful for investigation under adverse environmental conditions such as in the presence of water, oil or heavy vibration.

Refinements to the general technique allow the study of residual stresses, compressive stress fields, dynamic situations, plastic yielding and miniature components with little

increased difficulty. For a full treatment of these and other applications, the reader is referred to ref. 3.

16.2. Strain gauges

The accurate assessment of stresses, strains and loads in components under working conditions is an essential requirement of successful engineering design. In particular, the location of peak stress values and stress concentrations, and subsequently their reduction or removal by suitable design, has applications in every field of engineering. The most widely used experimental stress-analysis technique in industry today, particularly under working conditions, is that of strain gauges.

Whilst a number of different types of strain gauge are commercially available, this section will deal almost exclusively with the electrical resistance type of gauge introduced in 1939 by Ruge and Simmons in the United States.

The *electrical resistance strain gauge* is simply a length of wire or foil formed into the shape of a continuous grid, as shown in Fig. 16.5, cemented to a non-conductive backing. The gauge is then bonded securely to the surface of the component under investigation so that any strain in the surface will be experienced by the gauge itself. Since the fundamental equation for the electrical resistance R of a length of wire is

$$R = \frac{\rho L}{A} \tag{16.1}$$

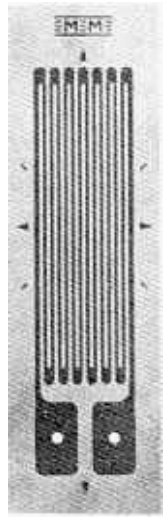

Fig. 16.5. Electric resistance strain gauge. (Welwyn Strain Measurement Ltd.)

where L is the length, A is the cross-sectional area and ρ is the *specific resistance* or *resistivity*, it follows that any change in length, and hence sectional area, will result in a change of resistance. Thus measurement of this resistance change with suitably calibrated equipment enables a direct reading of linear strain to be obtained. This is made possible by the

relationship which exists for a number of alloys over a considerable strain range between change of resistance and strain which may be expressed as follows:

$$\frac{\Delta R}{R} = K \times \frac{\Delta L}{L} \tag{16.2}$$

where ΔR and ΔL are the changes in resistance and length respectively and K is termed the *gauge factor.*
Thus

$$\text{gauge factor } K = \frac{\Delta R/R}{\Delta L/L} = \frac{\Delta R/R}{\varepsilon} \tag{16.3}$$

where ε is the strain. The value of the gauge factor is always supplied by the manufacturer and can be checked using simple calibration procedures if required. Typical values of K for most conventional gauges lie in the region of 2 to 2.2, and most modern strain-gauge instruments allow the value of K to be set accordingly, thus enabling strain values to be recorded directly.

The changes in resistance produced by normal strain levels experienced in engineering components are very small, and sensitive instrumentation is required. Strain-gauge instruments are basically *Wheatstone bridge* networks as shown in Fig. 16.6, the condition of balance for this network being (i.e. the galvanometer reading zero when)

$$R_1 \times R_3 = R_2 \times R_4 \tag{16.4}$$

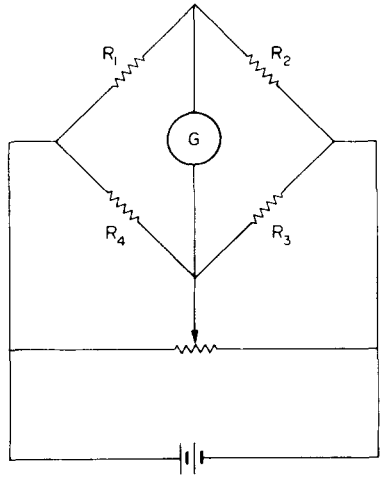

Fig. 16.6 Wheatstone bridge circuit.

In the simplest half-bridge wiring system, gauge 1 is the *active* gauge, i.e. that actually being strained. Gauge 2 is so-called *dummy* gauge which is bonded to an unstrained piece of metal similar to that being strained, its purpose being to cancel out any resistance change in R_1 that occurs due to temperature fluctuations in the vicinity of the gauges. Gauges 1 and 2 then represent the working half of the network – hence the name "half-bridge" system – and gauges 3 and 4 are standard resistors built into the instrument. Alternative wiring systems utilise one (*quarter-bridge*) or all four (*full-bridge*) of the bridge resistance arms.

16.3. Unbalanced bridge circuit

With the Wheatstone bridge initially balanced to zero any strain on gauge R_1 will cause the galvanometer needle to deflect. This deflection can be calibrated to read strain, as noted above, by including in the circuit an arrangement whereby gauge-factor adjustment can be achieved. Strain readings are therefore taken with the pointer off the zero position and the bridge is thus *unbalanced.*

16.4. Null balance or balanced bridge circuit

An alternative measurement procedure makes use of a variable resistance in one arm of the bridge to cancel any deflection of the galvanometer needle. This adjustment can then be calibrated directly as strain and readings are therefore taken with the pointer on zero, i.e. in the *balanced* position.

16.5. Gauge construction

The basic forms of wire and foil gauges are shown in Fig. 16.7. Foil gauges are produced by a printed-circuit process from selected melt alloys which have been rolled to a thin film, and these have largely superseded the previously popular wire gauge. Because of the increased area of metal in the gauge at the ends, the foil gauge is not so sensitive to strains at right angles to the direction in which the major axis of the gauge is aligned, i.e. it has a low transverse or cross-sensitivity – one of the reasons for its adoption in preference to the wire gauge. There are many other advantages of foil gauges over wire gauges, including better strain transmission from the substrate to the grid and better heat transmission from the grid to the substrate; as a result of which they are usually more stable. Additionally, the grids of foil gauges can be made much smaller and there is almost unlimited freedom of grid configuration, solder tab arrangement, multiple grid configuration, etc.

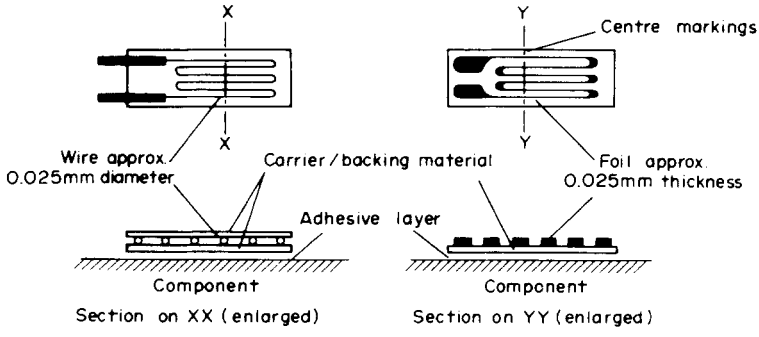

Fig. 16.7. Basic format of wire and foil gauges. (Merrow.)

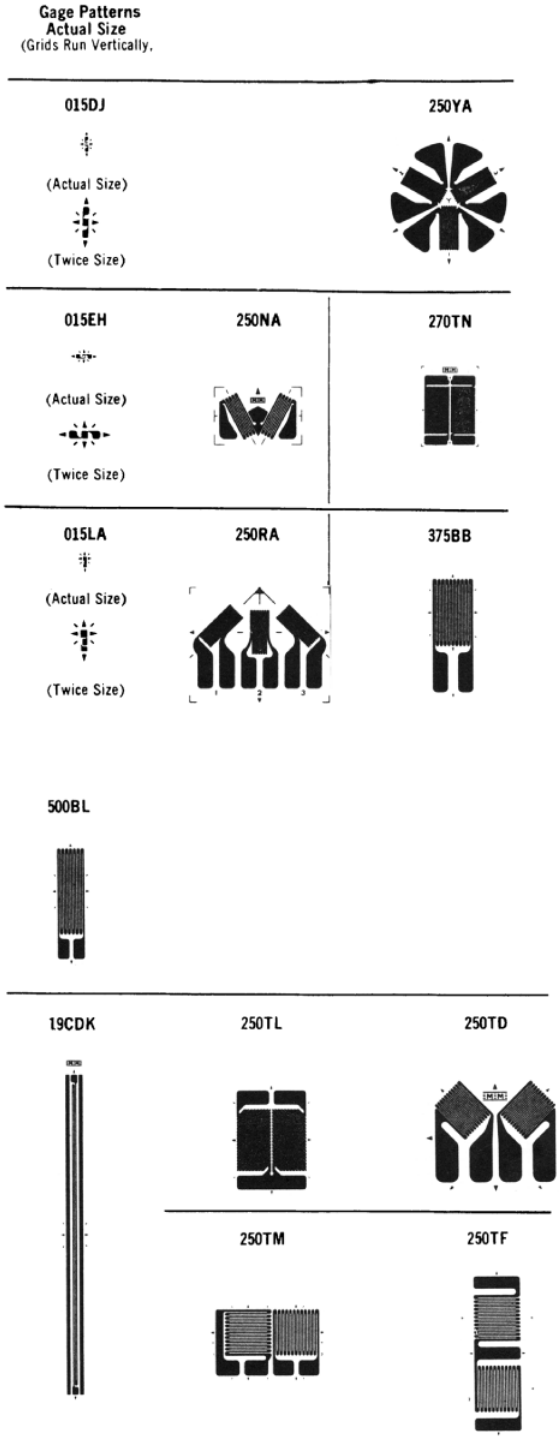

Fig. 16.8. Typical gauge sizes and formats. (Welwyn Strain Measurement Division.)

16.6. Gauge selection

Figure 16.8 shows but a few of the many types and size of gauge which are available. So vast is the available range that it is difficult to foresee any situation for which there is no gauge suitable. Most manufacturers' catalogues[13] give full information on gauge selection, and any detailed treatment would be out of context in this section. Essentially, the choice of a suitable gauge incorporates consideration of physical size and form, resistance and sensitivity, operating temperature, temperature compensation, strain limits, flexibility of the gauge backing (and hence relative stiffness) and cost.

16.7. Temperature compensation

Unfortunately, in addition to strain, other factors affect the resistance of a strain gauge, the major one being temperature change. It can be shown that temperature change of only a few degrees completely dwarfs any readings due to the typical strains encountered in engineering applications. Thus it is vitally important that any temperature effects should be cancelled out, leaving only the mechanical strain required. This is achieved either by using the conventional dummy gauge, *half-bridge*, system noted earlier, or, alternatively, by the use of *self-temperature-compensated gauges*. These are gauges constructed from material which has been subjected to particular metallurgical processes and which produce very small (and calibrated) thermal output over a specified range of temperature when bonded onto the material for which the gauge has been specifically designed (see Fig. 16.9).

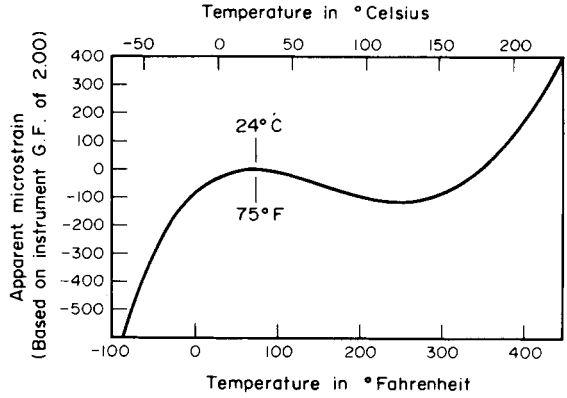

Fig. 16.9. Typical output from self-temperature-compensated gauge (Vishay).

In addition to the gauges, the lead-wire system must also be compensated, and it is normal practice to use the three-lead-wire system shown in Fig. 16.10. In this technique, two of the leads are in opposite arms of the bridge so that their resistance cancels, and the third lead, being in series with the power supply, does not influence the bridge balance. All leads must be of equal length and wound tightly together so that they experience the same temperature conditions.

In applications where a single self-temperature-compensated gauge is used in a quarter-bridge arrangement the three-wire circuit becomes that shown in Fig. 16.11. Again, only one of the current-carrying lead-wires is in series with the active strain gauge, the other is in series with the bridge completion resistor (occasionally still referred to as a "dummy") in the adjacent arm of the bridge. The third wire, connected to the lower solder tab of the active gauge, carries essentially no current but acts simply as a voltage-sensing lead. Provided the two lead-wires (resistance R_L) are of the same size and length and maintained at the same temperature (i.e. kept physically close to each other) then any resistance changes due to temperature will cancel.

16.8. Installation procedure

The quality and success of any strain-gauge installation is influenced greatly by the care and precision of the installation procedure and correct choice of the adhesive. The apparently mundane procedure of actually cementing the gauge in place is a critical step in the operation. Every precaution must be taken to ensure a chemically clean surface if perfect adhesion is to be attained. Full details of typical procedures and equipment necessary are given in refs 6 and

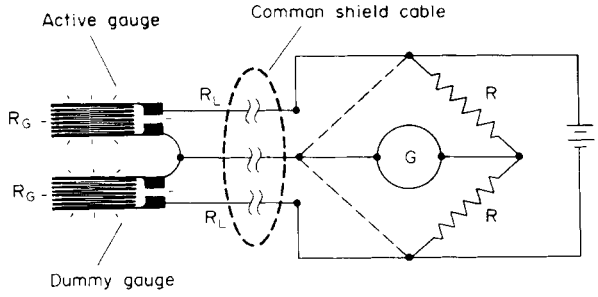

Fig. 16.10. Three-lead-wire system for half-bridge (dummy-active) operation.

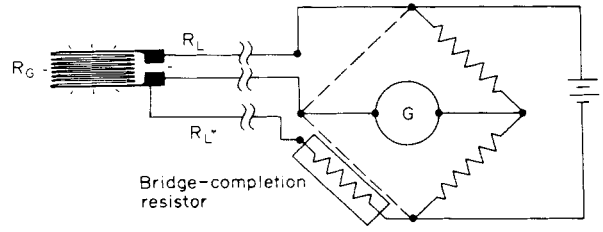

Fig. 16.11. Three-lead-wire system for quarter-bridge operation with single self-temperature-compensated gauge.

13, as are the methods which may be used to test the validity of the installation prior to recording measurements. Techniques for protection of gauge installations are also covered. Typical strain-gauge installations are shown in Figs. 16.12 and 16.13.

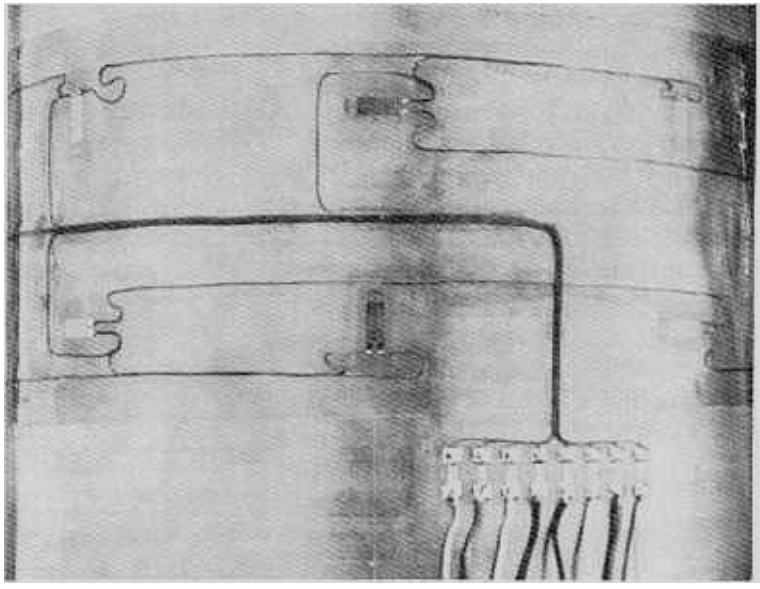

Fig. 16.12. Typical strain-gauge installation showing six of eight linear gauges bonded to the surface of a cylinder to record longitudinal and hoop strains. (Crown copyright.)

16.9. Basic measurement systems

(a) *For direct strain*

The standard procedure for the measurement of tensile or compressive direct strains utilises the *full-bridge* circuit of Fig. 16.14 in which not only are the effects of any bending eliminated but the sensitivity is increased by a factor of 2.6 over that which would be achieved using a single linear gauge.

Bearing in mind the balance requirement of the Wheatstone bridge, i.e. $R_1 R_3 = R_2 R_4$, each pair of gauges on either side of the equation will have an additive effect if their signs are similar or will cancel if opposite. Thus the opposite signs produced by bending cancel on both pairs whilst the similar signs of the direct strains are additive. The value 2.6 arises from twice the applied axial strain (R_1 and R_3) plus twice the Poisson's ratio strain (R_2 and R_4), assuming $\nu = 0.3$. The latter is compressive, i.e. negative, on the opposite side of the bridge from R_1 and R_3, and hence is an added signal to that of R_1 and R_3.

(b) *Bending*

Figure 16.15a shows the arrangement used to record bending strains independently of direct strains. It is normal to bond linear gauges on opposite surfaces of the component and to use the *half-bridge* system shown in Fig. 16.6; this gives a sensitivity of twice that which would be achieved with a single-linear gauge. Alternatively, it is possible to utilise again the Poisson strains as in §16.9(a) by bonding additional lateral gauges (i.e. perpendicular to the other

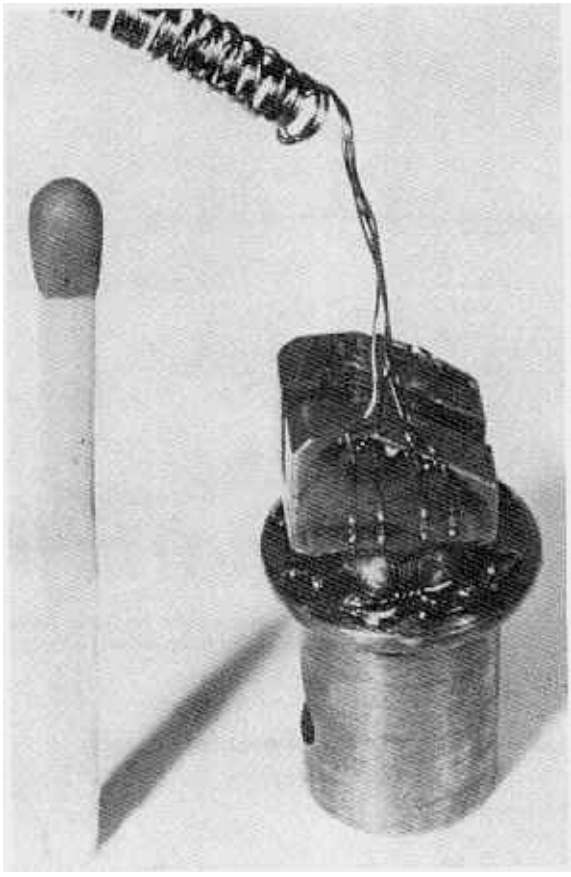

Fig. 16.13. Miniature strain-gauge installation. (Welwyn.)

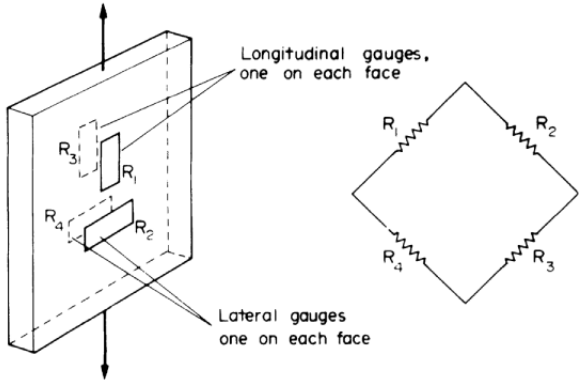

Fig. 16.14. "Full bridge" circuit arranged to eliminate any bending strains produced by unintentional eccentricities of loading in a nominal axial load application. The arrangement also produces a sensitivity 2.6 times that of a single active gauge. (Merrow.)

other gauges) on each surface and using a full-bridge circuit to achieve a sensitivity of 2.6. In this case, however, gauges R_2 and R_4 would be interchanged from the arrangement shown in Fig. 16.14 and would appear as in Fig. 16.15b.

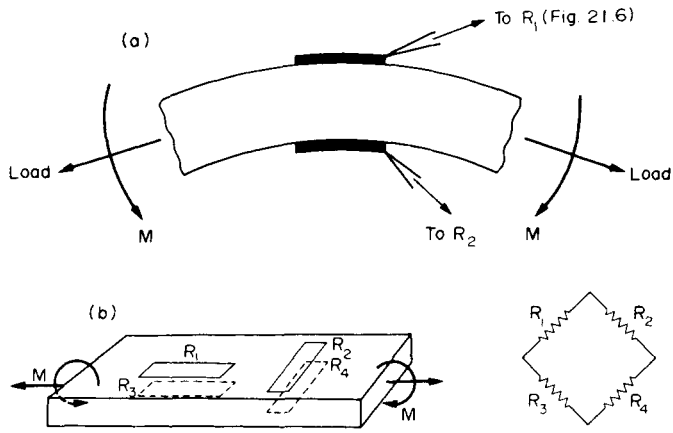

Fig. 16.15. (a) Determination of bending strains independent of end loads: "half-bridge" method. Sensitivity twice that of a single active gauge. (b) Determination of bending strains independent of end loads: "full-bridge" procedure. Sensitivity 2.6.

(*c*) *Torsion*

It has been shown that pure torsion produces direct stresses on planes at 45° to the shaft axis – one set tensile, the other compressive. Measurements of torque or shear stress using strain-gauge techniques therefore utilise gauges bonded at 45° to the axis in order to record the direct strains. Again, it is convenient to use a wiring system which automatically cancels unwanted signals, i.e. in this case the signals arising due to unwanted direct or bending strains which may be present. Once again, a full-bridge system is used and a sensitivity of four times that of a single gauge is achieved (Fig. 16.16).

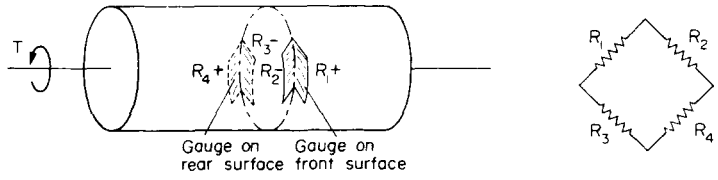

Fig. 16.16. Torque measurement using full-bridge circuit – sensitivity four times that of a single active gauge.

16.10. D.C. and A.C. systems

The basic Wheatstone bridge circuit shown in all preceding diagrams is capable of using either a direct current (d.c.) or an alternating current (a.c.) source; Fig. 16.6, for example,

shows the circuit excited by means of a standard battery (d.c.) source. Figure 16.17, however, shows a typical arrangement for a so-called a.c. *carrier frequency* system, the main advantage of this being that all unwanted signals such as noise are eliminated and a stable signal of gauge output is produced. The relative merits and disadvantages of the two types of system are outside the scope of this section but may be found in any standard reference text (refs. 4, 6, 7 and 13).

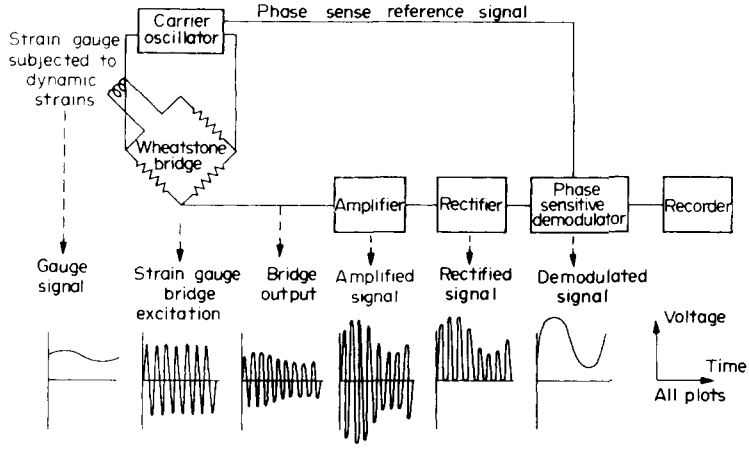

Fig. 16.17. Schematic arrangement of a typical carrier frequency system. (Merrow.)

16.11. Other types of strain gauge

The previous discussion has related entirely to the electrical resistance type of strain gauge and, indeed, this is by far the most extensively used type of gauge in industry today. It should be noted, however, that many other forms of strain gauge are available. They include:

(a) **mechanical gauges** or **extensometers** using optical or mechanical lever systems;
(b) **pneumatic gauges** using changes in pressure;
(c) **acoustic gauges** using the change in frequency of a vibrating wire;
(d) **semiconductor** or **piezo-resistive gauges** using the piezo-resistive effect in silicon to produce resistance changes;
(e) **inductance gauges** using changes in inductance of, e.g., differential transformer systems;
(f) **capacitance gauges** using changes in capacitance between two parallel or near-parallel plates.

Each type of gauge has a particular field of application in which it can compete on equal, or even favourable, terms with the electrical resistance form of gauge. None, however, are as versatile and generally applicable as the resistance gauge. For further information on each type of gauge the reader is referred to the references listed at the end of this chapter.

16.12. Photoelasticity

In recent years, photoelastic stress analysis has become a technique of outstanding importance to engineers. When polarised light is passed through a stressed transparent model, interference patterns or *fringes* are formed. These patterns provide immediate qualitative information about the general distribution of stress, positions of stress concentrations and of areas of low stress. On the basis of these results, designs may be modified to reduce or disperse concentrations of stress or to remove excess material from areas of low stress, thereby achieving reductions in weight and material costs. As photoelastic analysis may be carried out at the design stage, stress conditions are taken into account before production has commenced; component failures during production, necessitating expensive design modifications and re-tooling, may thus be avoided. Even when service failures do occur, photoelastic analysis provides an effective method of failure investigation and often produces valuable information leading to successful re-design. Typical photoelastic fringe patterns are shown in Fig. 16.18.

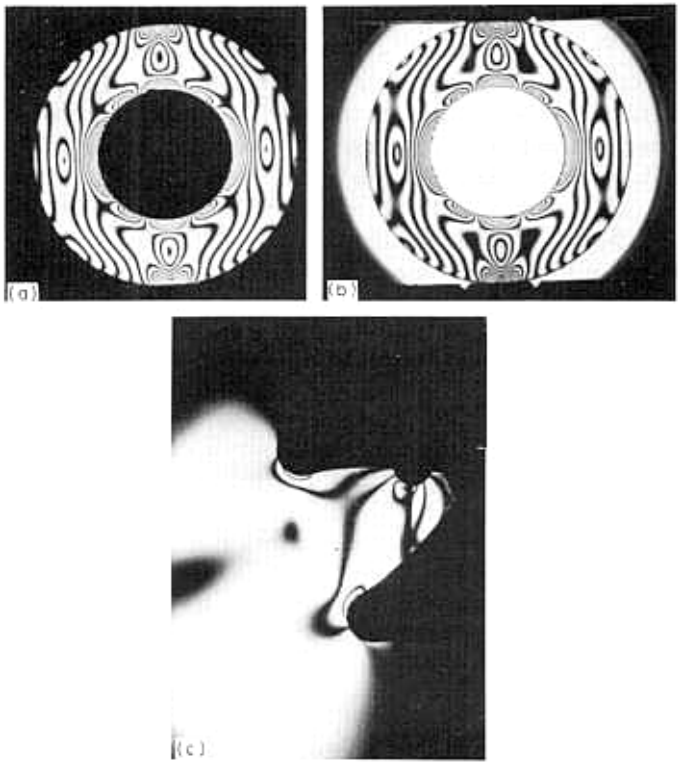

Fig. 16.18. Typical photoelastic fringe patterns. (a) Hollow disc subjected to compression on a diameter (dark field background). (b) As (a) but with a light field background. (c) Stress concentrations at the roots of a gear tooth.

Conventional or *transmission photoelasticity* has for many years been a powerful tool in the hands of trained stress analysts. However, untrained personnel interested in the technique have often been dissuaded from attempting it by the large volume of advanced mathematical

and optical theory contained in reference texts on the subject. Whilst this theory is, no doubt, essential for a complete understanding of the phenomena involved and of some of the more advanced techniques, it is important to accept that a wealth of valuable information can be obtained by those who are not fully conversant with all the complex detail. A major feature of the technique is that it allows one to effectively "look into" the component and pin-point flaws or weaknesses in design which are otherwise difficult or impossible to detect. Stress concentrations are immediately visible, stress values around the edge or boundary of the model are easily obtained and, with a little more effort, the separate principal stresses within the model can also be determined.

16.13. Plane-polarised light – basic polariscope arrangements

Before proceeding with the details of the photoelastic technique it is necessary to introduce the meaning and significance of *plane-polarised light* and its use in the equipment termed *polariscopes* used for photoelastic stress analysis. If light from an ordinary light bulb is passed through a polarising sheet or *polariser*, the sheet will act like a series of vertical slots so that the emergent beam will consist of light vibrating in one plane only: the plane of the slots. The light is then said to be *plane polarised.*

When directed onto an unstressed photoelastic model, the plane-polarised light passes through unaltered and may be completely extinguished by a second polarising sheet, termed an *analyser*, whose axis is perpendicular to that of the polariser. This is then the simplest form of polariscope arrangement which can be used for photoelastic stress analysis and it is termed a *"crossed" set-up* (see Fig. 16.19). Alternatively, a *"parallel" set-up* may be used in which the axes of the polariser and analyser are parallel, as in Fig. 16.20. With the model unstressed, the plane-polarised light will then pass through both the model and analyser unaltered and maximum illumination will be achieved. When the model is stressed in the parallel set-up, the resulting fringe pattern will be seen against a light background or "field", whilst with the crossed arrangement there will be a completely black or "dark field".

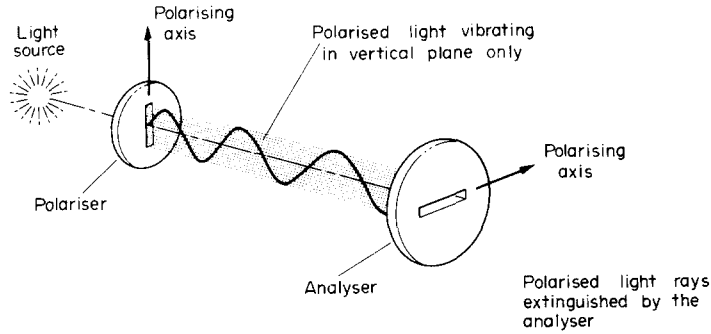

Fig. 16.19. "Crossed" set-up. Polariser and analyser arranged with their polarising axes at right angles; plane polarised light from the polariser is completely extinguished by the analyser. (Merrow.)

16.14. Temporary birefringence

Photoelastic models are constructed from a special class of transparent materials which exhibit a property known as *birefringence*, i.e. they have the ability to split an incident plane-

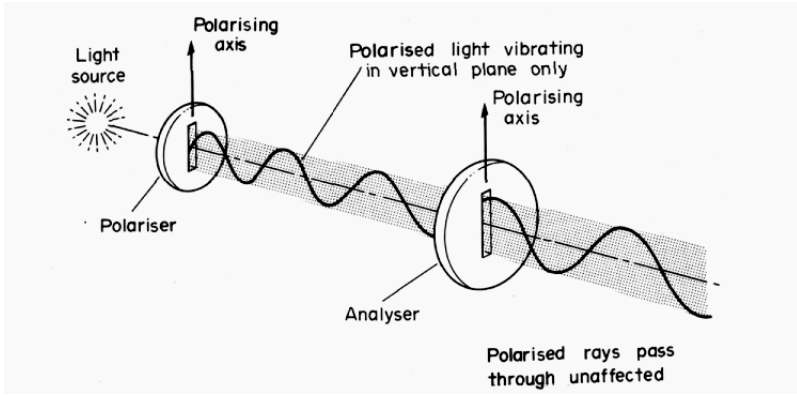

Fig. 16.20. "Parallel" set-up. Polariser and analyser axes parallel; plane-polarised light from the polariser passes through the analyser unaffected, producing a so-called "light field" arrangement. (Merrow.)

polarised ray into two component rays; they are *double refracting*. This property is only exhibited when the material is under stress, hence the qualified term "*temporary birefringence*", and the direction of the component rays always coincides with the directions of the principal stresses (Fig. 16.21). Further, the speeds of the rays are proportional to the magnitudes of the respective stresses in each direction, so that the rays emerging from the model are out of phase and hence produce interference patterns when combined.

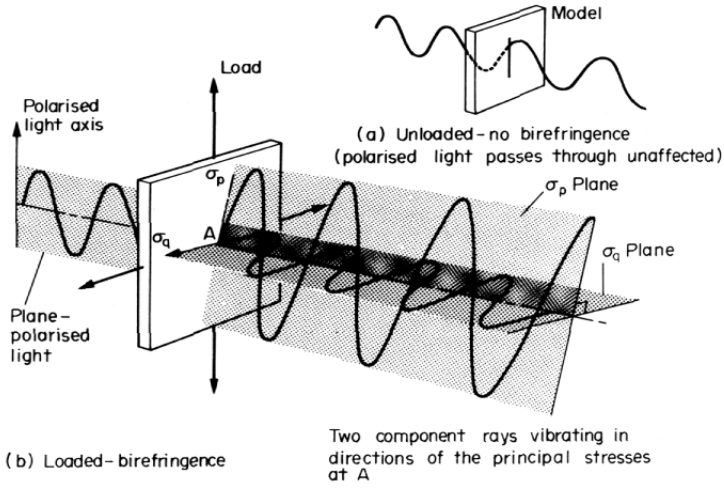

Fig. 16.21. Temporary birefringence. (a) Plane-polarised light directed onto an unstressed model passes through unaltered. (b) When the model is stressed the incident plane-polarised light is split into two component rays. The directions of the rays coincide with the directions of the principal stresses, and the speeds of the rays are proportional to the magnitudes of the respective stresses in their directions. The emerging rays are out of phase, and produce an interference pattern of fringes. (Merrow.)

16.15. Production of fringe patterns

When a model of an engineering component constructed from a birefringent material is stressed, it has been shown above that the incident plane-polarised light will be split into two component rays, the directions of which at any point coincide with the directions of the principal stresses at the point. The rays pass through the model at speeds proportional to the principal stresses in their directions and emerge out of phase. When they reach the analyser, shown in the crossed position in Fig. 16.22, only their horizontal components are transmitted and these will combine to produce interference fringes as shown in Fig. 16.23.

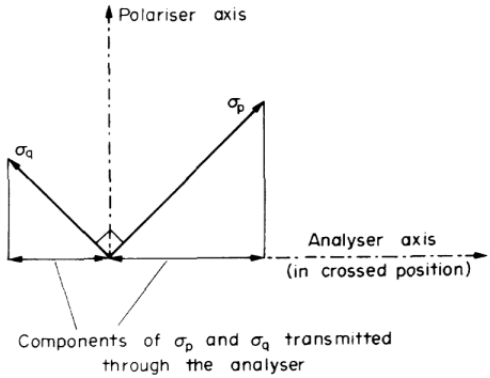

Fig. 16.22. Transmission through the analyser. (Merrow.)

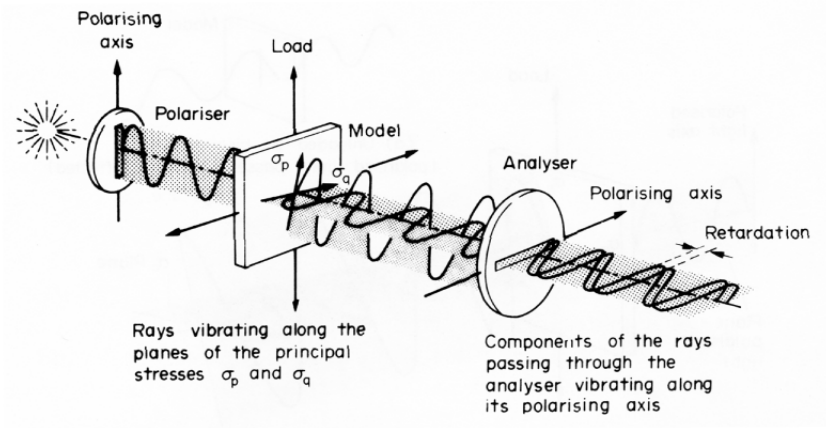

The difference in speeds of the rays, and hence the amount of interference produced, is proportional to the difference in the principal stress values $(\sigma_p - \sigma_q)$ at the point in question. Since the maximum shear stress in any two-dimensional stress system is given by

$$\tau_{max} = \tfrac{1}{2}(\sigma_p - \sigma_q)$$

it follows that the interference or fringe pattern produced by the photoelastic technique will give an immediate indication of the variation of shear stress throughout the model. Only at a free, unloaded boundary of a model, where one of the principal stresses is zero, will the fringe pattern yield a direct indication of the principal direct stress (in this case the tangential boundary stress). However, since the majority of engineering failures are caused by fatigue cracks commencing at the point of maximum tensile stress at the boundary, this is not a severe limitation. Further discussion of the interpretation of fringe patterns is referred to the following section.

If the original light source is *monochromatic*, e.g. mercury green or sodium yellow, the fringe pattern will appear as a series of distinct black lines on a uniform green or yellow background. These black lines or fringes correspond to points where the two rays are exactly 180° out of phase and therefore cancel. If white light is used, however, each composite wavelength of the white light is cancelled in turn and a multicoloured pattern of fringes termed *isochromatics* is obtained.

Monochromatic sources are preferred for accurate quantitative photoelastic measurements since a high number of fringes can be clearly discerned at, e.g., stress concentration positions. With a white light source the isochromatics become very pale at high stress regions and clear fringe boundaries are no longer obtained. White light sources are therefore normally reserved for general qualitative assessment of models, for isolation of zero fringe order positions (i.e. zero shear stress) which appear black on the multicoloured background, and for the investigation of stress directions using *isoclinics*. These are defined in detail in §16.19.

16.16. Interpretation of fringe patterns

It has been stated above that the pattern of fringes achieved by the photoelastic technique yields:

(a) *A complete indication of the variation of shear stress throughout the entire model.* Since ductile materials will generally fail in shear rather than by direct stress, this is an important feature of the technique. At points where the fringes are most numerous and closely spaced, the stress is highest; at points where they are widely spaced or absent, the stress is low. With a white-light source such areas appear black, indicating zero shear stress, but it cannot be emphasised too strongly that this does not necessarily mean zero stress since if the values of σ_p and σ_q (however large) are equal, then $(\sigma_p - \sigma_q)$ will be zero and a black area will be produced. Extreme care must therefore be taken in the interpretation of fringe patterns. Generally, however, fringe patterns may be compared with contour lines on a map, where close spacing relates to steep slopes and wide spacing to gentle inclines. Peaks and valleys are immediately evident, and actual heights are readily determined by counting the contours and converting to height by the known scale factor. In an exactly similar way, photoelastic fringes are counted from the known zero (black) positions and the resulting number or order of fringe at the point in question is converted to stress by a calibration constant known as the *material fringe value*. Details of the calibration procedure will be given later.

(b) *Individual values of the principal stresses at free unloaded boundaries, one of these always being zero.* The particular relevance of this result to fatigue failures has been mentioned, and the use of photoelasticity to produce modifications to boundary profiles in order to reduce boundary stress concentrations and hence the likelihood of fatigue failures has been a major

use of the technique. In addition to the immediate indication of high stress locations, the photoelastic model will show regions of low stress from which material can be conveniently **removed** without weakening the component to effect a reduction in weight and material cost. Surprisingly, perhaps, a reduction in material at or near a high stress concentration can also produce a significant reduction in maximum stress. Re-design can be carried out on a "file-it-and-see" basis, models being modified or re-shaped within minutes in order to achieve the required distribution of stress.

Whilst considerable valuable qualitative information can be readily obtained from photoelastic models without any calculations at all, there are obviously occasions where the precise values of the stresses are required. These are obtained using the following basic equation of photoelasticity,

$$\sigma_p - \sigma_q = \frac{nf}{t} \tag{16.5}$$

where σ_p and σ_q are the values of the maximum and minimum principal stresses at the point under consideration, n is the fringe number or *fringe order* at the point, f is the *material fringe value* or *coefficient*, and t is the model thickness.

Thus with a knowledge of the material fringe value obtained by calibration as described below, the required value of $(\sigma_p - \sigma_q)$ at any point can be obtained readily by simply counting the fringes from zero to achieve the value n at the point in question and substitution in the above relatively simple expression.

Maximum shear stress or boundary stress values are then easily obtained and the application of one of the so-called *stress-separation* procedures will yield the separate value of the principal stress at other points in the model with just a little more effort. These may be of particular interest in the design of components using brittle materials which are known to be relatively weak under the action of direct stresses.

16.17. Calibration

The value of f, which, it will be remembered, is analogous to the height scale for contours on a survey map, is determined by a simple calibration experiment in which the known stress at some point in a convenient model is plotted against the fringe value at that point under various loads. One of the most popular loading systems is diametral compression of a disc, when the relevant equation for the stress at the centre is

$$\sigma_p - \sigma_q = \frac{8P}{\pi Dt} \tag{16.6}$$

where P is the applied load, D is the disc diameter and t is the thickness.

Thus, comparing with the photoelastic equation (16.5),

$$\frac{nf}{t} = \frac{8P}{\pi Dt}$$

The slope of the load versus fringe order graph is given by

$$\frac{P}{n} = f \times \frac{\pi D}{8} \tag{16.7}$$

Hence f can be evaluated.

16.18. Fractional fringe order determination – compensation techniques

The accuracy of the photoelastic technique is limited, among other things, to the accuracy with which the fringe order at the point under investigation can be evaluated. It is not sufficiently accurate to count to the nearest whole number of fringes, and precise determination of fractions of fringe order at points lying between fringes is required. Conventional methods for determining these fractions of fringe order are termed *compensation techniques* and allow estimation of fringe orders to an accuracy of one-fiftieth of a fringe. The two methods most often used are the Tardy and Senarmont techniques. Before either technique can be adopted, the directions of the polariser and analyser must be aligned with the directions of the principal stresses at the point. This is achieved by rotating both units together in the plane polariscope arrangement until an *isoclinic* (§16.19) crosses the point. In most modern polariscopes facilities exist to couple the polariser and analyser together in order to facilitate synchronous rotation. The procedure for the two techniques then varies slightly.

(a) *Tardy method*

Quarter-wave plates are inserted at 45° to the polariser and analyser as the dark field circular polariscope set-up of Fig. 16.24. Normal fringe patterns will then be visible in the absence of isoclinics.

(b) *Senarmont method*

The polariser and analyser are rotated through a further 45° retaining the dark field, thus moving the polarising axes at 45° to the principal stress directions at the point. Only one quarter-wave plate is then inserted between the model and the analyser and rotated to again achieve a dark field. The normal fringe pattern is then visible as with the Tardy method.

Thus, having identified the integral value n of the fringe order at the point, i.e. between 1 and 2, or 2 and 3, for instance, the fractional part can now be established for both methods in the same way.

The analyser is rotated on its own to produce movement of the fringes. In particular, the nearest *lower order* of fringe is moved to the point of interest and the angle θ moved by the analyser recorded.

The fringe order at the chosen point is then $n + \dfrac{\theta^\circ}{180^\circ}$.

N.B. – Rotation of the analyser in the opposite direction ϕ° would move the nearest *highest order* fringe $(n+1)$ back to the point. In this case the fringe order at the point would be

$$(n+1) - \frac{\phi}{180}$$

It can be shown easily by trial that the sum of the two angles θ and ϕ is always 180°.

There is little to choose between the two methods in terms of accuracy; some workers prefer to use Tardy, others to use Senarmont.

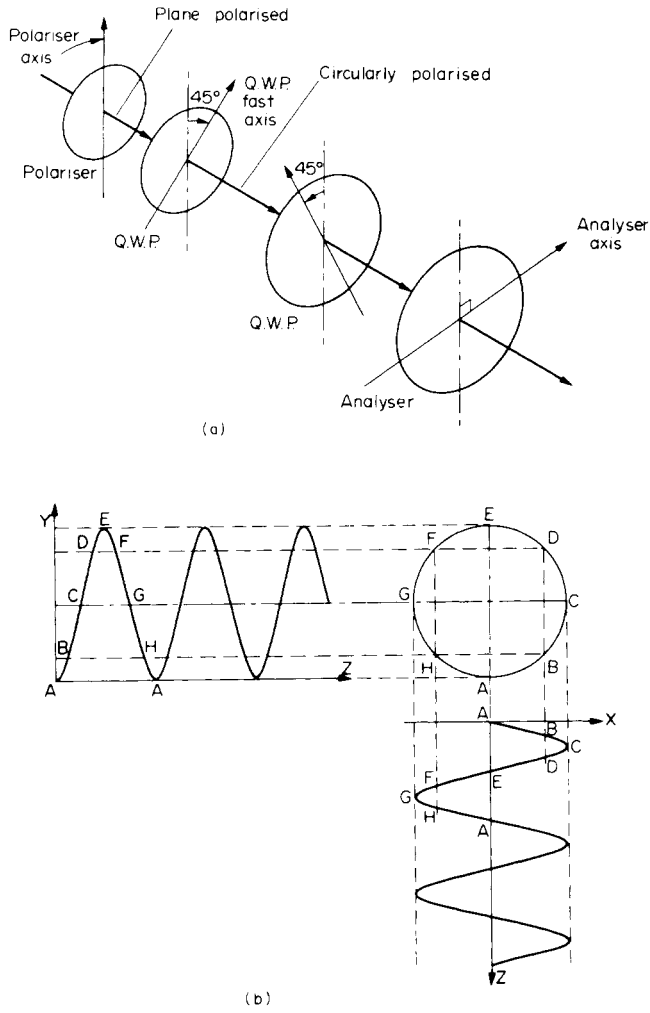

Fig. 16.24. (a) Circular polariscope arrangement. Isoclinics are removed optically by inserting quarter-wave plates (Q.W.P.) with optical axes at 45° to those of the polariser and analyser. Circularly polarised light is produced. (Merrow.) (b) Graphical construction for the addition of two rays at right angles a quarter-wavelength out of phase, producing resultant circular envelope, i.e. circularly polarised light.

16.19. Isoclinics – circular polarisation

If plane-polarised light is used for photoelastic studies as suggested in the preceding text, the fringes or isochromatics will be partially obscured by a set of black lines known as isoclinics (Fig. 16.25). With the coloured isochromatics of a white light source, these are easily identified, but with a monochromatic source confusion can easily arise between the black fringes and the black isoclinics.

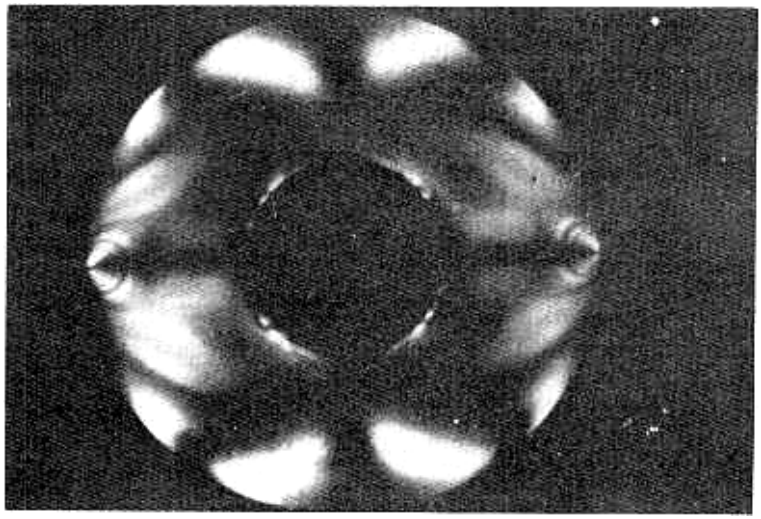

Fig. 16.25. Hollow disc subjected to diametral compression as in Fig. 16.18a but in this case showing the isoclinics superimposed.

It is therefore convenient to use a different optical system which eliminates the isoclinics but retains the basic fringe pattern. The procedure adopted is outlined below.

An *isoclinic* line is a locus of points at which the principal stresses have the same inclination; the 20° isoclinic, for example, passes-through all points at which the principal stresses are inclined at 20° to the vertical and horizontal (Fig. 16.26). Thus isoclinics are not peculiar to photoelastic studies; it is simply that they have a particular relevance in this case and they are readily visualised. For the purpose of this introduction it is sufficient to note that they are used as the basis for construction of *stress trajectories* which show the directions of the principal stresses at all points in the model, and hence in the component. Further details may be found in the relevant standard texts.

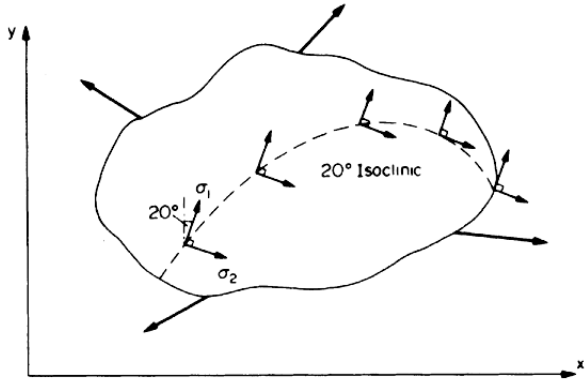

Fig. 16.26. The 20° isoclinic in a body subjected to a general stress system. The isoclinic is given by the locus of all points at which the principal stresses are inclined at 20° to the reference x and y axes.

To prevent the isoclinics interfering with the analysis of stress magnitudes represented by the basic fringe pattern, they are removed optically by inserting quarter-wave plates with their axes at 45° to those of the polariser and analyser as shown in Fig. 16.24. These eliminate all unidirectional properties of the light by converting it into *circularly polarised* light. The amount of interference between the component rays emerging from the model, and hence the fringe patterns, remains unchanged and is now clearly visible in the absence of the isoclinics.

16.20. Stress separation procedures

The photoelastic technique has been shown to provide principal stress difference and hence maximum shear stresses at all points in the model, boundary stress values and stress directions. It has also been noted that there are occasions where the separate values of the principal stresses are required at points other than at the boundary, e.g. in the design of components using brittle materials. In this case it is necessary to employ one of the many *stress separation* procedures which are available. It is beyond the scope of this section to introduce these in detail, and full information can be obtained if desired from standard texts.[8, 9, 11] The principal techniques which find most application are (a) the oblique incidence method, and (b) the shear slope or "shear difference" method.

16.21. Three-dimensional photoelasticity

In the preceding text, reference has been made to models of uniform thickness, i.e. two-dimensional models. Most engineering problems, however, arise in the design of components which are three-dimensional. In such cases the stresses vary not only as a function of the shape in any one plane but also throughout the "thickness" or third dimension. Often a proportion of the more simple three-dimensional model or loading cases can be represented by equivalent two-dimensional systems, particularly if the models are symmetrical, but there remains a greater proportion which cannot be handled by the two-dimensional approach. These, however, can also be studied using the photoelastic method by means of the so-called *stress-freezing* technique.

Three-dimensional photoelastic models constructed from the same birefringent material introduced previously are loaded, heated to a critical temperature and cooled very slowly back to room temperature. It is then found that a fringe pattern associated with the elastic stress distribution in the component has been locked or "frozen" into the model. It is then possible to cut the model into thin slices of uniform thickness, each slice then being examined as if it were a two-dimensional model. Special procedures for model manufacture, slicing of the model and fringe interpretation are required, but these are readily obtained with practice.

16.22. Reflective coating technique[12]

A special adaptation of the photoelastic technique utilises a thin sheet of photoelastic material which is bonded onto the surface of a metal component using a special adhesive containing an aluminium pigment which produces a reflective layer. Polarised light is directed onto the photoelastic coating and viewed through an analyser after reflection off the metal surface using a *reflection polariscope* as shown in Fig. 16.27.

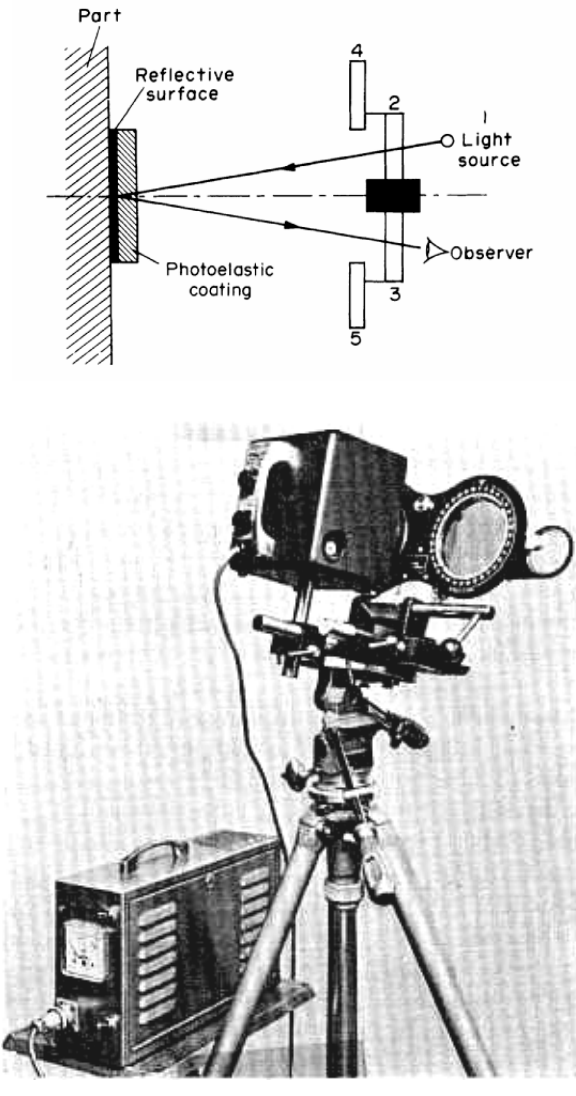

Fig. 16.27. Reflection polariscope principle and equipment.

A fringe pattern is observed which relates to the strain in the metal component. The technique is thus no longer a model technique and allows the evaluation of strains under loading conditions. Static and dynamic loading conditions can be observed, the latter with the aid of a stroboscope or high-speed camera, and the technique gives a full field view of the strain distribution in the surface of the component. Unlike the transmission technique, however, it gives no information as to the stresses *within* the material.

Standard photoelastic sheet can be used for bonding to flat components, but special casting techniques are available which enable the photoelastic material to be obtained in a partially polymerised, very flexible, stage, and hence allows it to be contoured or moulded around complex shapes without undue thickness changes. After a period has been allowed for

complete polymerisation to occur in the moulded position, the sheet is removed and bonded firmly back into place with the reflective adhesive.

The reflective technique is particularly useful for the observation of service loading conditions over wide areas of structure and is often used to highlight the stress concentration positions which can subsequently become the subject of detailed strain-gauge investigations.

16.23. Other methods of strain measurement

In addition to the widely used methods of experimental stress analysis or strain measurement covered above, there are a number of lesser-used techniques which have particular advantages in certain specialised conditions. These techniques can be referred to under the general title of grid methods, although in some cases a more explicit title would be "interference methods".

The standard **grid technique** consists of marking a grid, either mechanically or chemically, on the surface of the material under investigation and measuring the distortions of this grid under strain. A direct modification of this procedure, known as the **"replica" technique**, involves the firing of special pellets from a gun at the grid both before and during load. The surface of the pellets are coated with "Woods metal" which is heated in the gun prior to firing. Replicas of the undeformed and deformed grids are then obtained in the soft metal on contact with the grid-marked surface. These are viewed in a vernier comparison microscope to obtain strain readings.

A further modification of the grid procedure, known as the **moiré technique**, superimposes the deformed grid on an undeformed master (or vice versa). An interference pattern, known as **moiré fringes**, similar to those obtained when two layers of net curtain are superimposed, is produced and can be analysed to yield strain values.

X-rays can be used to obtain surface strain values from measurements of crystal lattice deformation. **Acoustoelasticity**, based on a principle similar to photoelasticity but using polarised ultrasonic sound waves, has been proposed but is not universally accepted to date. **Holography**, using the laser as a source of coherent light, and again relying on the interference obtained between holograms of deformed and undeformed components, has recently created considerable interest, but none of these techniques appear at the moment to represent a formidable challenge to the major techniques listed earlier.

Bibliography

1. A. J. Durelli, E. A. Phillips and C. H. Tsao, *Analysis of Stress and Strain*, McGraw-Hill, New York, 1958.
2. Magnaflux Corporation, *Principles of Stresscoat.*
3. E. J. Hearn, *Brittle Lacquers for Strain Measurement*, Merrow Publishing Co., Watford, England, 1971.
4. C. C. Perry and H. P. Lissner, *Strain Gauge Primer*, McGraw-Hill, New York.
5. T. Potma, *Strain Gauges*, Iliffe, London, 1967.
6. E. J. Hearn, *Strain Gauges*, Merrow Publishing Co., Watford, England, 1971.
7. R. Murray and P. Stein, *Strain Gauge Techniques*, M.I.T. Press, Cambridge, Mass., 1956.
8. E. J. Hearn, *Photoelasticity*, Merrow Publishing Co., Watford, England, 1971.
9. M. M. Frocht, *Photoelasticity*, vols. I and II, Wiley, 1961.
10. H. T. Jessop and F. C. Harris, *Photoelasticity*, Cleaver-Hume, 1949.
11. E. G. Coker and L. N. G. Filon, *Photoelasticity*, Cambridge University Press, 1957.
12. F. Zandman, S. Redner, J. W. Dally, *Photoelastic Coatings* Iowa State/S.E.S.A. 1977.
13. J. Pople/B.S.S.M. *Strain Measurement Reference Book.* B.S.S.M. Newcastle, England.